# The Genome-Wide Expression Profile of *Nelumbinis semen* on Lipopolysaccharide-Stimulated BV-2 Microglial Cells

Sung-Hwa Sohn,[a] Hwan-Suck Chung,[a] Eunjung Ko,[a] Hyuk-joon Jeong,[a] Sung-Hoon Kim,[b] Jin-Hyun Jeong,[c] Yangseok Kim,[a] Minkyu Shin,[a] Moochang Hong,[a] and Hyunsu Bae*,[a]

[a] *Department of Physiology, College of Oriental Medicine, Kyung Hee University;* [b] *Department of Oriental Pathology, College of Oriental Medicine, Kyung Hee University; and* [c] *College of Pharmacy, Kyung Hee University; Seoul 130–701, Republic of Korea.* Received February 2, 2009; accepted March 24, 2009; published online March 27, 2009

**This study was conducted to evaluate the protective mechanisms of *Nelumbinis semen* (NS) on lipopolysaccharide (LPS)-induced activation of BV-2 microglial cells. The anti-inflammatory effects of NS were determined by analyzing nitric oxide production and proinflammatory cytokines using enzyme-linked immunosorbent assay. The mechanism was evaluated in BV-2 cells with or without NS treated with LPS for various lengths of time using oligonucleotide microarray and real time reverse transcription-polymerase chain reaction. The oligonucleotide microarray analysis revealed that mitogen activated protein kinase (MAPK) signaling pathway-related genes such as *Fgfr3*, *Fgf12*, *Rasal2*, *Nfkb2*, *Map2k5*, *Mapk1*, *Map3k7*, and *NFatc2* were down-regulated in LPS activated BV-2 cells by pretreatment with NS. In addition, significant decreases in *Nos1ap* gene expression were observed with NS pretreatment. Cluster linked pathway analysis using the Kyoto Encyclopedia of Genes and Genomes database revealed that the effects of NS were closely associated with the regulation of mitochondria functions. These results suggested that NS can affect the MAPK signaling pathway and mitochondrial functions in BV-2 cells activated with LPS.**

**Key words** *Nelumbinis semen*; gene expression profile; anti-inflammatory effect; microarray

It has been suggested that microglia, which are the resident macrophage-like population of brain cells, play a role in host defense and tissue repair in the central nervous system (CNS). These cells constitute the first line of defense against infection and injury in the brain.[1,2] Active microglia release a variety of pro-inflammatory mediators such as cytokines, prostanoids, and complement components, as well as potentially neurotoxic substances such as reactive oxygen species (ROS), nitric oxide (NO) and excitatory amino acids.[3—8] NO plays an important role in a variety of physiological processes, including smooth muscle relaxation, platelet inhibition, neurotransmission, immune responses and inflammation; however, NO is known to be an important mediator of acute and chronic inflammation.[9] Therefore, inhibition of microglial activation would be an effective therapeutic approach to alleviating the progression of neuroinflammatory diseases including Alzheimer's and Parkinson's disease.[6,10,11]

During the screening of products produced by medicinal plants for new therapeutic agents for the treatment of inflammation and neurodegenerative diseases, the inhibitory activities of 270 spray-dried extracts of herbal medicines on LPS-induced NO production in BV-2 microglial cells were evaluated. Among these extracts, *Nelumbinis semen* (NS) showed the highest inhibitory activity, therefore this compound was selected for this study. NS, or lotus seed, had been widely used for the treatment of cardiovascular symptoms, insomnia, anxiety, post-menopausal depression, anti-depression, anti-oxidation, and hepatoprotection.[12—14] In addition, NS has radical scavenging activity.[15] Natural products have long been used in traditional medicine to treat inflammation and other inflammation-related diseases, and the raw materials of these products are often used to develop new drugs.[16—18] Many factors contribute to the appeal of herbal medicine and claims that herbs may both treat and prevent diseases. These claims add to the belief that these treatments are safe because they are a natural, gentle, and therefore a harmless alternative to conventional medicine.

Microarray analysis is a molecular technique that enables the parallel analysis of gene expression by a very large number of genes encompassing a significant fraction of the human genome. This method is both qualitative and quantitative because it is able to detect changes in the levels of expression in treated cells based on comparison with control samples.[19,20] Therefore, the use of microarray analysis allows development of more advanced therapies for the treatment of inflammatory disease using naturally derived products.

The goal of this study was to determine the protective mechanisms of NS on LPS-induced activation in BV-2 microglial cells. We evaluated the effects of NS on LPS treated microglial cells to determine if NS prevented activation of the cells. The results of these tests and the possible mechanisms by which they occurred are discussed herein.

## MATERIALS AND METHODS

**Preparation of NS** NS (Lot No. 151301 (Expiration date 01/14/2010), 111201 (Expiration date 12/10/2009)) was purchased from Sun Ten Pharmaceutical (Taipei, Taiwan) and made in to a powder. 0.1 g was extracted by stirring in 10 ml of distilled water (DW) overnight at room temperature. The sample was then centrifuged for 10 min at 3000 rpm, after which the supernatant was removed and sterilized by passing it through a 0.22 $\mu$m syringe filter and then used for the experiments.

**Cell Culture** The immortalized murine BV-2 microglial cell line, which exhibits both the phenotypic and functional properties of reactive microglia cells, were kindly provided by Dr. S. Go (Kyung Hee University, Seoul, Korea) and maintained in 100% humidity and 5% $CO_2$ at 37 °C in DMEM supplemented with 10% fetal bovine serum (FBS), streptomycin, and penicillin (Invitrogen Life Technologies,

* To whom correspondence should be addressed. e-mail: hbae@khu.ac.kr

© 2009 Pharmaceutical Society of Japan

Rockville, U.S.A.). BV-2 microglial cells were then plated onto 100 mm, flat-bottom tissue culture plates at a density of $1\times10^7$ cells/ml in hormonally defined DMEM media as described previously. The medium was changed every 2 d until the cells became 80—90% confluent, at which point they were used for experiments. Mixed glial cultures were prepared from cerebral cortices of 3—5 d-old Bl/C57 mice according to the method of Giulian and Baker.[21] After mechanical and chemical dissociation, cortical cells were seeded in DMEM-F12 with 10% FBS. Medium was replaced every 4—5 d and confluencecy was achieved after 10—12 d *in vitro*.

**Nitric Oxide Assay** The level of nitrate measured by a Griess reaction was taken as a measure of NO production. Briefly, cells were plated at a density of $1\times10^6$ cells/well in 1 ml of DMEM medium. Cells were then treated with 0.01, 0.1, and 1 $\mu$g/ml NS or left un-treated, and then incubated for 30 min at 37 °C. LPS (1 $\mu$g/ml) (Sigma, St. Louis, MO, U.S.A.) was then added to the cultures, which were then incubated for additional 24 h at 37 °C. Next, 100 $\mu$l of cell free culture supernatant was combined with 100 $\mu$l of Griess reagent (Sigma, St. Louis, MO, U.S.A.). The samples were then incubated for 10 min at room temperature, after which the absorbance at 540 nm was determined using a microplate reader (Molecular Devices, Sunnyvale, CA, U.S.A.).

**Cytokine Assays** Cells were plated at a density of $1\times10^6$ cells/well in 1 ml of DMEM medium for 4 h, after which they were treated with 0.01, 0.1, or 1 $\mu$g/ml NS or left untreated. Next, the samples were incubated for an additional 30 min, after which 1 $\mu$g/ml LPS was added to the samples. The cells were then re-incubated at 37 °C for 24 h, after which the cell free culture supernatants were collected. The supernatants were analyzed for cytokines by ELISA (OptEIA TNF-$\alpha$ Mouse Set, BD Bioscience, San Jose, CA, U.S.A.). Briefly, flat-bottom 96-well plates were coated with anti-mouse TNF-$\alpha$ and incubated overnight at 4 °C. The antibody was then discarded and the plates were blocked with assay diluents (BD Bioscience, San Jose, CA, U.S.A.) for 1 h at room temperature. These plates were then washed three times with wash buffer (0.05% Tween 20 in PBS) and blotted on a paper towel. Next, diluted samples and standards were added in triplicate and the plates were then incubated for 2 h at room temperature. The supernatant was then discarded, after which the wells were washed five times with wash buffer. Next, TNF-$\alpha$ detecting antibody plus Avidin-HRP was added to the samples, which were then incubated for 1 h at room temperature. The plates were then washed, after which tetramethylbenzidine substrate solution (Pharmingen, SanDiego, CA, U.S.A.) was added. The color was allowed to develop for 30 min in the dark before the reaction was quenched with a stop solution (0.2 N $H_2SO_4$).

**Cell Viability Assay** Cell growth was measured by an 5-(3-carboxymethoxyphenyl)-2-(4,5-dimethylthiazoly)-3-(4-sulfophenyl)tetrazolium, inner salt (MTS) assay using the Cell Titer 96® Aqueous One Solution Cell Proliferation Assay Kit (Promega, Madison, WI, U.S.A.). The MTS assay was performed as described by Chung *et al.*[18] with some modifications. For the cell viability assays, were the cells pretreated with NS for 30 min and then exposed to LPS for 24 h, the media was removed and 100 $\mu$l of fresh media was added, followed by the addition of 20 $\mu$l of MTS solution. The plates were then incubated at 37 °C for 1 h in a humidified (5% $CO_2$) environment, after which the absorbance at 490 nm was read using a microplate reader (Molecular Devices, Sunnyvale, CA, U.S.A.).

**RNA Preparation** BV-2 microglial cells were initially cultured in a 100 mm dish ($1\times10^7$/ml) for 24 h, and then pretreated with 1 $\mu$g/ml NS or left untreated. The cells were then incubated for 30 min, after which 1 $\mu$g/ml LPS was added. Next, the cells were incubated at 37 °C for 30 min, 1 h, 3 h, or 6 h. The RNA was then isolated from the BV-2 microglial cells using an Rneasy® mini kit (Qiagen GmbH, Hilden, Germany) according to the manufacturer's instructions, after which the RNA was quantified using a NanoDrop (NanoDrop Technologies, Inc., ND-1000; Wilmington, DE, U.S.A.).

**Oligonucleotide Chip Microarray** Oligonucleotide chip microarray was performed using single round RNA amplification protocols, following the Affymetrix specifications (Affymetrix GeneChip Expression Analysis Technical Manual). Briefly, 3 $\mu$g of total RNA were used to synthesize first-strand complementary DNA (cDNA) using oligonucleotide probes with 24 oligo-dT plus T7 promoter as primers (Proligo LLC, Boulder, CO, U.S.A.) and the Superscript Choice System (Life Technologies, Invitrogen, Milan, Italy). After double-stranded cDNA synthesis, the products were purified by phenol–chloroform extraction, and then biotinylated antisense complimentary RNA (cRNA) was generated through *in vitro* transcription using a BioArray RNA High-Yield Transcript Labeling Kit (ENZO Life Sciences Inc., Farmingdale, NY, U.S.A.). The biotinylated labeled cRNA was then fragmented, and 10 $\mu$g of the total fragmented cRNA was hybridized to the Affymetrix Mouse 430 2.0 GeneChip array (P/N900470, Affymetrix Inc., U.S.A.). The Affymetrix Fluidics Station 400 was then used to wash and stain the chips, after which the nonhybridized target was removed. Next, the samples were incubated with a streptavidin–phycoerythrin conjugate to stain the biotinylated cRNA. The staining was then amplified using goat IgG as blocking reagent and biotinylated antistreptavidin antibody (goat), followed by a second staining step using a streptavidin–phycoerythrin conjugate. The fluorescence was detected using the Genechip System Confocal Scanner (Hewlett-Packard), and analysis of the data contained on each GeneChip was conducted using the GeneChip 3.1 software produced by Affymetrix, using the standard default settings. To compare different chips, global scaling was used, with all probe sets being scaled to a user-defined target intensity of 150.

**Data Analysis** The Beadstudio v3.0 was used to evaluate the expression signals generated by the Affymetrix Mouse 430 2.0 array. Global scaling normalization was then performed and the normalized data were log-transformed using base 2. Next, fold change and a Welch *t*-test were applied to select the differentially expressed genes (DEGs) using a fold change threshold of 2.0-fold and a $p<0.05$ to indicate significance. Each probe set used in the Affymetrix GeneChip produces a detection call, with P (present call) indicating good quality, M (marginal call) indicating intermediate quality and A (absent call) indicating relatively low reliability. Therefore, probe sets that resulted in A calls in the compared groups were removed to filter false positives. A volcano plot was used to better visualize and compare the

two DEG methods. The 2.0-fold DEGs were clustered using the GenPlex™ v2.8 software (ISTECH Inc., Korea) using hierarchical clustering with Pearson correlation as a similarity measure and complete linkage as the linkage method). In addition, gene ontology significance analysis was conducted to investigate the functional relationships among the 2.0-fold DEGs using high-throughput GoMiner. The 2.0-fold DEGs were then mapped to relevant pathways using GenPlex™ v2.8 software (ISTECH Inc., Korea). The pathway resources were provided by the KEGG database. Samples were compared to extract regulated genes between LPS-treated and control (non-treated) BV-2 cells. And samples were compared to extract regulated genes between LPS plus NS-treated and LPS-treated BV-2 cells.

**Real Time RT-PCR Analysis** Microarray verification was performed by real time RT-PCR analysis of selected genes using SYBR Green I Master Mix (Applied Biosystems, Foster City, CA, U.S.A.) and primers (Genotech Inc., Korea). Complementary DNA (cDNA) was synthesized using 2 $\mu$g of RNA in a reverse transcription reaction. Real time-PCR quantitative mRNA analyses were performed with an Applied Biosystems 7300 Real Time PCR System using the SYBR Green fluorescence quantification system (Applied Biosystems, Foster City, CA, U.S.A.) to quantify the amplicons. The PCR conditions were 40 cycles of 95 °C (15 s), 60 °C (1 min), and a standard denaturation curve. The sequences of the mouse primers were as follows: Nos1ap (forward primer 5′-cca ttc agt gag cat gga gg-3′; reverse primer 5′-aac cct tcc cta ggc ttt cc-3′), Mapk1 (forward primer 5′-ggc tgg cct caa act cta cc-3′; reverse primer 5′-agc atc cca gca gca ata aa-3′), Nfatc2 (forward primer 5′-gga gag aca aga cat gga cagc-3′; reverse primer 5′-ctc cat gaa cac aac ctt gga-3′), Map2k5 (forward primer 5′-ctg aat cct gct ctc ccc at-3′; reverse primer 5′-taa ttt cca gct cca tcc cc-3′), and GAPDH (forward primer 5′-ttc acc acc atg gag aag gc-3′; reverse primer 5′-ggc atg gac tgt ggt cat ga-3′). PCR conditions for each target were optimized according to the primer concentration, the absence of primer dimer formation, and the efficiency of amplification of both the target genes and the housekeeping gene control. PCR reactions were carried out in a total volume of 20 $\mu$l in PCR master mix containing 10 $\mu$l 2X SYBR Green, 5 $\mu$M each of sense and antisense primer, and 2 $\mu$l of 1 : 2 diluted cDNA to a final volume of 20 $\mu$l with DEPC-treated $H_2O$. To normalize the cDNA content of the samples, we used the comparative threshold ($C_T$) cycle method, which consists of the normalization of the number of target gene copies *versus* the endogenous reference gene, GAPDH. The $C_T$ is defined as the fractional cycle number at which the fluorescence generated by cleavage of the probe passes a fixed threshold baseline when amplification of the PCR product is first detected.

**Blood–Brain Barrier (BBB) Penetration Analysis** BBB analysis was conducted using the PreADMET program (Web-based PreADMET, http://preadmet.bmdrc.org). Blood–brain barrier (BBB) penetration is represented as BB= [Brain]/[Blood], where [Brain] and [Blood] are the steady-state concentration of radiolabled compounds in brain and peripheral blood.

**Statistical Analysis** Statistical analysis of the data was conducted using the Prism 3.02 software (GraphicPad Software Inc., CA, U.S.A.). Data were analyzed by one-way ANOVA for multiple comparisons. One-way ANOVA was performed to compare values and post-test was done by Tukey's multiple comparison test. Results with a $p<0.05$ were considered statistically significant.

## RESULTS

**Nitric Oxide Assay** We investigated secretion of NO in NS (0.01, 0.1, or 1 $\mu$g/ml) treated BV-2 microglial cells by Griess reagent kit analysis. Figure 1 shows that NS can down-regulate NO secretion in a dose-dependent manner. Especially, NO secretion was decreased significantly by 30% in response to treatment with 1 $\mu$g/ml NS.

**Cytokine Assays** The secretion of TNF-$\alpha$ was measured in BV-2 microglial cells and primary microglial cells at NS (0.01, 0.1, or 1 $\mu$g/ml) treatment. Figure 2 shows that NS can down-regulated TNF-$\alpha$ secretion in a dose-dependent manner. TNF-$\alpha$ secretion was decreased significantly by 30% after treatment with 1 $\mu$g/ml NS in BV-2 microglial cells (Fig. 2A). Especially, TNF-$\alpha$ secretion was decreased significantly by 60% after treatment with 1 $\mu$g/ml NS in primary microglial cells (Fig. 2B).

**Cell Viability of BV-2 Microglial Cells** To determine the cytotoxicity effect of NS LPS-induced activation in BV-2 microglial cells, we investigated cell viability using an MTS assay. Treatment with NS did not exert a cytotoxic effect on BV-2 microglial cells (Fig. 3).

**Gene Expression Profiles in BV-2 Microglial Cells** Gene expression profiles were significantly up- or down-regulated in the experimental groups (LPS or LPS plus NS-treated BV-2 microglial cells) when compared with the control (non-treated BV-2 microglial cells). In total, 1654 differentially expressed genes (27%) were detected in the experimental group using approximately 45100 oligonucleotide probes. For the experimental group, genes showing highly altered expression levels were aligned according to the magnitude of the altered expression. Most of the differentially expressed genes (111) are listed in Table 1, which shows a comparison of the expression levels for a variety of genes between the experimental group and the control. All genes were grouped into functional categories and metabolic pathways based on the Kyoto Encyclopedia of Genes and Genomes

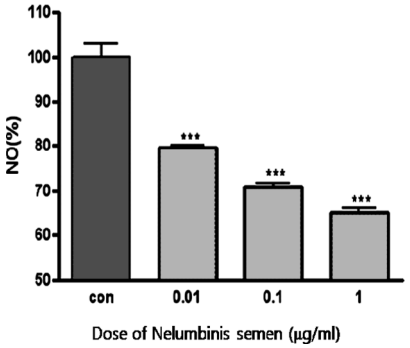


Fig. 1. Dose-Dependent Inhibitory Effects of *Nelumbinis semen* on Production of Nitric Oxide Induced by LPS in BV2 Cells

Con: untreated BV-2 microglial cells. The values were normalized in proportion to the value of control; $n=3$ (each group). One-way ANOVA was performed to compare values and post-test was done by Tukey's multiple comparison test. Values are mean±standard deviation (S.D.) Three tailed probability value of <0.001 was considered significant. *** $p<0.001$, compared to control group.

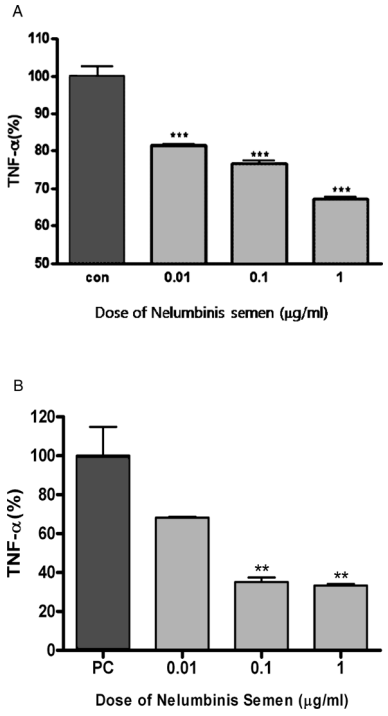


Fig. 2. Dose-Dependent Inhibitory Effects of *Nelumbinis semen* on Production of TNF-$\alpha$ Induced by LPS in BV2 (A) and Primary Microglial Cells (B)

Con: untreated BV-2 and primary microglial. The values were normalized in proportion to the value of control; $n=3$ (each group). One-way ANOVA was performed to compare values and post-test was done by Tukey's multiple comparison test. Values are mean±S.D. Three tailed probability value of $<0.001$ was considered significant. $^{**}p<0.01$ and $^{***}p<0.001$, compared to control group.

(KEGG) database. To understand the molecular mechanism of NS in LPS-treated cells, a hierarchical clustering algorithm was used to group genes on the basis of similar expression patterns (Fig. 4). Each row in Fig. 4 represents the hybridization results for a single set of oligonucleotide probes in the array, and each column represents the expression levels of all genes in a single hybridization sample. The expression level of each gene was visualized in color, relative to its median expression level compared with that of control. Red represents an expression level greater than the control, green represents an expression level less than the control expression level and the color intensity denotes the degree of deviation from the control. The cells included in this map include samples from both the experimental group and the control. Coordinately expressed genes are grouped into clusters, which are named according to the cellular process in which they participate. The clustergram revealed that up- or down-regulated genes were grouped into functional categories (Fig. 4). Furthermore, the clustergram revealed that clusters of genes related to 40 signaling pathways are up- and down-regulated in the cells pretreated with NS and then stimulated with LPS (Table 2). These pathways are listed in ascending order by *p*-value, so that those at the top of the list have the smallest *p*-values. To assess the reliability of our microarray technique, we calculated the microarray reproducibility between triplicate RNA samples from three independent cell cultures. The correlation matrix plot from the control (non-treated), LPS-treated and LPS plus NS-treated BV-2 cells showed in Fig. 5. A good relationship between triplicates

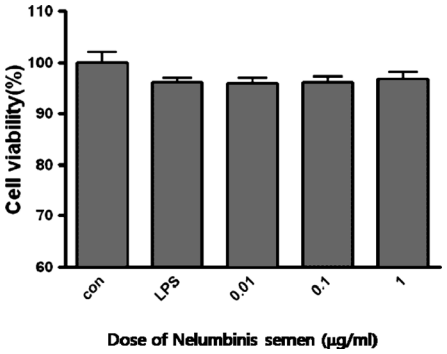


Fig. 3. Effect of *Nelumbinis semen* on the Cell Viability and Cytotoxicity in LPS-Stimulated BV-2 Microglial Cells

BV-2 microglial cells were treated with NS (0.01, 0.1, or 1 $\mu$g/ml) for 30 min and then stimulated with 1 $\mu$g/ml LPS for 24 h. Con: untreated, LPS: only LPS-treated BV-2 microglial cells. The values of cell viability were normalized in proportion to the value of control; $n=3$ (each group).

would be a slope of 1.

**Validation of Selected Genes *via* Real Time RT-PCR** The SYBR Green assay was used to confirm expression changes of 5 selected genes, *Nos1ap*, *Mapk1*, *Nfatc2*, *Map2k5* and *Nfkb2* identified by microarray analysis in the pretreated with NS in LPS-treated BV-2 cells. The real-time RT-PCR assay yielded results that showed qualitative agreement with the microarray results (Fig. 6).

**Blood–Brain Barrier (BBB) Analysis of NS** In order to predict if chemicals in NS could pass through the blood–brain barrier (BBB), *in silico* BBB penetration analysis was performed. Among 19 chemicals reportedly found in NS,[22—24] three chemicals were predicted as central nervous system active compound based on the classification reported by Lobell *et al*.[25] These three compounds included $\beta$-sitosterol glucopyranoside, armepavine and neferine with brain/blood ratio of 5.304, 0.9931 and 0.47760 respectively.

## DISCUSSION

Microglia is the major cell type involved in neuroinflammatory events in brain diseases such as encephalitis, stroke, and neurodegenerative disorders.[26,27] Therefore, the inhibitory activities of 270 herbal medicines on LPS-induced NO and TNF-$\alpha$ production in BV-2 microglial cells were evaluated in an effort to find new therapeutic agents for the treatment of neuroinflammation diseases (data not shown). The results of this analysis revealed that NS showed considerable inhibitory activity, with 30% inhibition at a concentration of 1 $\mu$g/ml being observed (Figs. 1, 2A). Especially, NS showed 60% inhibition at a concentration of 1 $\mu$g/ml in primary microglial cells (Fig. 2B). In addition, *in silico* BBB penetration analysis predicts that there are at least three compounds in NS could possibly pass through BBB and thus act on microglia cells. Therefore, NS was selected for further study to evaluate the inhibition mechanisms by which it exerted its effects on LPS-induced NO and TNF-$\alpha$ production in BV-2 microglial cells. However, the early signaling events involved in LPS-induced microglial activation are not completely understood, therefore we evaluated the gene expression profiles of BV-2 microglial cells. The cells were pretreated with NS for 30 min and then LPS for (0.5, 1, 3, or 6 h).

Table 1. Alteration in Gene Expression in LPS Stimulated BV-2 Microglial Cells with and without *Nelumbinis semen* Pretreatment

| Genes | Symbol | Regulation profile and average $\log_2$ fold change | | | | | | | |
|---|---|---|---|---|---|---|---|---|---|
| | | LPS[a)] | | | | NS/LPS[a)] | | | |
| | | 30 m | 1 h | 3 h | 6 h | 30 m | 1 h | 3 h | 6 h |
| Endocytosis-related genes | | | | | | | | | |
| Formin binding protein 1 | Fnbp1 | 1.7 | 3.9 | 5.1 | 3.3 | −1.7 | −2.1 | −1.5 | −2.5 |
| Signal transduction-related genes | | | | | | | | | |
| CD247 antigen | Cd247 | 2.1 | 0.9 | 3.0 | 2.9 | −0.2 | −1.9 | −3.4 | −1.9 |
| Centaurin, delta 1 | Centd1 | −1.9 | −3.2 | −2.0 | −0.6 | −1.1 | 4.8 | 2.0 | 1.1 |
| v-crk sarcoma virus CT10 oncogene homolog (avian)-like | Crkl | 2.5 | 2.8 | 3.3 | 2.7 | −0.2 | −2.9 | −2.5 | −1.9 |
| CXXC finger 4 | Cxxc4 | −3.2 | −3.0 | −1.1 | −2.7 | 3.1 | 2.0 | 0.6 | 2.4 |
| Discoidin domain receptor family, member 1 | Ddr1 | −0.7 | −1.7 | −1.9 | −1.1 | 0.8 | 2.0 | 2.4 | 2.9 |
| Predicted gene, EG665317 | EG665317 | 1.5 | 2.2 | 2.3 | 3.0 | −2.2 | −1.7 | −0.9 | −2.3 |
| Estrogen receptor 1 (alpha) | Esr1 | −0.2 | −2.5 | −3.0 | −2.8 | −0.3 | 2.8 | 1.7 | 2.6 |
| Fibroblast growth factor 12 | Fgf12 | −0.2 | 2.8 | 4.4 | 3.7 | −1.1 | −2.3 | −1.9 | −1.1 |
| Fibroblast growth factor receptor 3 | Fgfr3 | 3.3 | 3.8 | 3.7 | 3.1 | −0.8 | −1.1 | −2.5 | −1.5 |
| Follicle stimulating hormone beta | Fshb | −0.6 | 3.8 | 1.4 | 3.0 | 1.2 | −4.0 | −1.0 | −2.1 |
| Glycine receptor, alpha 1 subunit | Glra1 | 2.6 | 2.2 | 2.6 | 1.8 | −0.7 | −2.1 | −1.9 | −1.1 |
| Guanine nucleotide binding protein, alpha stimulating, olfactory type | Gnal | 3.1 | 3.9 | 3.8 | 4.0 | −1.2 | −3.9 | −1.4 | −2.0 |
| G protein-coupled receptor 149 | Gpr149 | −2.3 | −2.9 | −3.2 | −1.7 | 0.7 | 2.1 | 4.7 | 1.4 |
| Mitogen activated protein kinase kinase 5 | Map2k5 | −0.1 | 0.3 | 0.8 | 0.2 | −0.8 | −1.3 | −1.0 | −0.5 |
| Mitogen activated protein kinase kinase kinase 7 | Map3k7 | 0.3 | 0.1 | 0.1 | 0.0 | −1.4 | −1.1 | −1.1 | −1.1 |
| Mitogen-activated protein kinase kinase kinase kinase 4 | Map4k4 | −0.2 | 0.3 | 0.1 | 0.3 | −1.0 | −1.6 | −1.0 | −1.1 |
| Mitogen activated protein kinase 1 | Mapk1 | 1.4 | 0.7 | 1.9 | 1.2 | −2.9 | −2.4 | −3.6 | −2.7 |
| Mitogen activated protein kinase 8 interacting protein 1 | Mapk8ip1 | 2.6 | 3.6 | 2.6 | 0.7 | 0.8 | −1.5 | −1.9 | −0.5 |
| Nuclear factor of activated T-cells, cytoplasmic, calcineurin-dependent 2 | Nfatc2 | 1.2 | 0.9 | 0.8 | 2.2 | 0.0 | −0.4 | −0.4 | −1.7 |
| Nuclear factor of kappa light polypeptide gene enhancer in B-cells 2, p49/p100 | Nfkb2 | 0.2 | 0.7 | 1.1 | 1.0 | −0.4 | −0.4 | −0.8 | −0.2 |
| Phosphodiesterase 4B, cAMP specific | Pde4b | −0.2 | 2.8 | 2.0 | 2.0 | 0.4 | −2.2 | −2.2 | −1.6 |
| Prokineticin receptor 1 | Prokr1 | −2.2 | −2.4 | −1.8 | −0.1 | 4.3 | 3.9 | 1.8 | 0.3 |
| RAS protein activator like 2 | Rasal2 | 1.6 | 0.7 | 2.2 | 1.6 | −4.1 | −5.1 | −2.5 | −3.5 |
| Regulator of G-protein signaling 12 | Rgs12 | −1.1 | −2.5 | −2.3 | −2.1 | −0.6 | 1.0 | 2.1 | 2.1 |
| Sortilin-related VPS10 domain containing receptor 3 | Sorcs3 | −0.8 | −3.0 | −1.5 | −3.0 | 1.8 | 4.0 | 2.1 | 3.5 |
| Spleen tyrosine kinase | Syk | 1.4 | 2.4 | 2.5 | 2.2 | −3.5 | −1.7 | −1.4 | −2.4 |
| Transforming growth factor, beta receptor II | Tgfbr2 | 0.4 | 0.6 | 1.2 | 1.2 | −0.3 | −0.4 | −3.1 | −1.8 |
| Tensin 3 | Tns3 | 1.8 | 2.1 | 1.9 | 2.2 | −3.4 | −1.8 | −2.7 | −1.9 |
| TNF receptor-associated factor 6 | Traf6 | 0.7 | 0.7 | −0.1 | 0.8 | 0.0 | −1.9 | −0.3 | −0.8 |
| Tribbles homolog 1 (Drosophila) | Trib1 | −2.8 | −2.9 | −1.7 | −0.6 | 2.8 | 3.7 | 1.8 | 0.9 |
| Wingless-related MMTV integration site 5B | Wnt5b | −2.9 | −2.1 | −2.4 | −2.2 | 0.2 | 1.7 | 0.6 | 1.3 |
| Apoptosis-related genes | | | | | | | | | |
| Bcl2 modifying factor | Bmf | −0.4 | −2.9 | −1.8 | −3.2 | 1.0 | 3.9 | 1.4 | 2.6 |
| CASP8 and FADD-like apoptosis regulator | Cflar | 0.2 | 0.9 | 2.1 | 2.2 | −1.2 | −1.4 | −1.6 | −1.9 |
| Granzyme B | Gzmb | 2.6 | 2.5 | 2.7 | 1.1 | −1.5 | −1.2 | −1.2 | −1.0 |
| GPI anchor biosynthesis-related genes | | | | | | | | | |
| CDC91 cell division cycle 91-like 1 (*S. cerevisiae*) | Cdc91l1 | 3.1 | 3.5 | 4.0 | 3.7 | −0.3 | −2.8 | −1.4 | −0.6 |
| Phosphatidylinositol glycan anchor biosynthesis, class Q | Pigq | 2.2 | 2.7 | 2.3 | 1.7 | −1.6 | −0.3 | −2.6 | −1.6 |
| Cellular defense response-related genes | | | | | | | | | |
| T-cell receptor beta, variable 13 | Tcrb-V13 | 4.0 | 3.6 | 3.5 | 4.2 | −1.6 | −2.8 | −1.7 | −3.0 |
| Ttranscription-related genes | | | | | | | | | |
| RIKEN cDNA 1110033M05 gene | 1110033M05Rik | 2.2 | 1.7 | 3.5 | 2.9 | −3.5 | −2.9 | −6.1 | −1.4 |
| cAMP responsive element binding protein 3-like 2 | Creb3l2 | 1.8 | 1.7 | 3.6 | 1.9 | −2.2 | −1.0 | −2.0 | −1.9 |
| CREB binding protein | Crebbp | 0.3 | 0.6 | 0.7 | −0.7 | −4.0 | −3.2 | −1.1 | −2.7 |
| Developing brain homeobox 2 | Dbx2 | −4.4 | −3.3 | −0.7 | −4.1 | 3.3 | 4.3 | 2.0 | 0.8 |
| Fer3-like (Drosophila) | Ferd3l | 3.6 | 2.2 | 3.2 | 3.0 | −2.6 | −1.7 | −2.5 | −0.7 |
| Homeo box B9 | Hoxb9 | −3.7 | −3.2 | −3.1 | −2.3 | 2.0 | 1.7 | 3.4 | −0.7 |
| Jun proto-oncogene related gene d1 | Jund1 | 0.1 | 0.2 | 0.3 | 0.2 | −1.3 | −1.2 | −1.2 | −1.1 |
| Myelin transcription factor 1-like | Myt1l | −0.8 | −3.4 | −1.9 | −3.6 | 2.0 | 4.1 | 2.7 | 0.8 |
| Nuclear factor I/X | Nfix | 2.1 | 2.8 | 2.7 | 0.5 | −17 | −2.8 | −1.9 | −0.3 |
| Naked cuticle 2 homolog (Drosophila) | Nkd2 | 4.1 | 2.5 | 2.2 | 2.9 | −0.3 | −1.0 | −2.4 | −2.6 |
| Receptor-interacting serine-threonine kinase 4 | Ripk4 | 2.2 | 3.3 | 0.2 | 3.0 | −1.9 | −2.0 | −1.3 | −3.3 |
| RAR-related orphan receptor alpha | Rora | −2.8 | −1.8 | −2.8 | −2.5 | 2.6 | 2.0 | 3.3 | 1.5 |
| SERTA domain containing 2 | Sertad2 | 2.0 | 2.8 | 2.9 | 1.8 | −1.4 | −1.3 | −4.0 | −2.8 |
| Simple repeat sequence-containing transcript | Srst | −0.7 | −4.2 | −3.7 | −2.3 | −2.0 | 0.9 | 3.3 | 2.7 |
| Wilms tumor homolog | Wt1 | −0.2 | −1.3 | −2.0 | −2.9 | 0.6 | 2.1 | 2.9 | 4.2 |
| Metabolism-related genes | | | | | | | | | |
| Lipase, endothelial | Lipg | 5.3 | 4.2 | 5.4 | 4.4 | −3.1 | −1.4 | −0.3 | −0.8 |
| Phosphatidylinositol glycan anchor biosynthesis, class N | Pign | −4.1 | −4.0 | −2.1 | −2.4 | 2.4 | 3.6 | 2.0 | 3.3 |
| Phospholipase A2, group VI | Pla2g6 | −0.6 | −4.1 | −1.6 | −0.6 | 1.7 | 4.9 | 2.7 | 1.7 |
| Polyribonucleotide nucleotidyltransferase 1 | Pnpt1 | 1.6 | 1.9 | 2.1 | 2.1 | −1.8 | −1.9 | −2.5 | −2.1 |
| Orphan short chain dehydrogenase/reductase | Sdro | 2.9 | 2.4 | 3.6 | 2.3 | −2.0 | −1.1 | −3.0 | −1.3 |
| Transport-related genes | | | | | | | | | |
| ATP-binding cassette, sub-family C(CFTR/MRP), member 6 | Abcc6 | −1.0 | −2.0 | −1.6 | −3.2 | −1.7 | 0.3 | 2.0 | 2.1 |
| ATPase, (Na+)/K+ transporting, beta 4 polypeptide | Atp1b4 | −0.6 | −5.4 | −4.6 | −4.9 | −1.2 | 2.8 | 2.2 | 3.9 |
| Cystic fibrosis transmembrane conductance regulator homolog | Cftr | −3.3 | −4.7 | −4.8 | −3.9 | 2.8 | 5.1 | 4.6 | 2.7 |

Table 1. (continued)

| Genes | Symbol | Regulation profile and average $\log_2$ fold change | | | | | | | |
|---|---|---|---|---|---|---|---|---|---|
| | | LPS[a)] | | | | NS/LPS[a)] | | | |
| | | 30 m | 1 h | 3 h | 6 h | 30 m | 1 h | 3 h | 6 h |
| Cytochrome P450, family 2, subfamily a, polypeptide 4 | Cyp2a4 | 4.2 | 4.4 | 4.5 | 3.4 | −4.3 | −2.7 | −1.9 | −2.2 |
| Cytochrome P450, family 2, subfamily b, polypeptide 10 | Cyp2b10 | −3.0 | −2.8 | −1.6 | −0.9 | 5.2 | 2.5 | 3.6 | 2.1 |
| Gap junction membrane channel protein alpha 8 | Gja8 | −2.8 | −3.6 | −3.8 | −3.3 | 1.9 | 2.7 | 0.7 | 2.2 |
| Glutamate receptor, ionotropic, kainate 4 | Grik4 | −2.7 | −2.5 | −2.9 | −2.7 | 1.7 | 2.5 | 0.9 | 0.6 |
| Lipocalin 4 | Lcn4 | 2.3 | 1.7 | 2.0 | 2.5 | −0.2 | −1.4 | −2.0 | −3.3 |
| Orosomucoid 1 | Orm1 | −1.8 | −2.9 | −2.8 | −1.4 | 2.3 | 3.4 | 4.1 | −1.0 |
| Solute carrier family 10, member 2 | Slc10a2 | 3.5 | 3.8 | 3.4 | 3.7 | −2.2 | −3.2 | −3.3 | −2.3 |
| Solute carrier family 18 (vesicular monoamine), member 1 | Slc18a1 | −0.7 | 2.3 | 3.4 | 4.0 | 1.0 | −1.7 | −1.9 | −1.1 |
| Synaptotagmin XVII | Syt17 | −3.4 | −4.0 | −1.6 | −2.7 | 1.5 | 2.0 | 2.8 | 2.6 |
| Transmembrane 9 superfamily member 2 | Tm9sf2 | 2.5 | 2.4 | 1.7 | 2.7 | −4.0 | −2.1 | −2.6 | −4.8 |
| Translocase of outer mitochondrial membrane 20 homolog | Tomm20 | −2.6 | −2.9 | −2.3 | −2.4 | 0.8 | 2.7 | 0.6 | 3.2 |
| Ubiquitously transcribed tetratricopeptide repeat gene, Y chromosome | Uty | −3.5 | −3.1 | −2.4 | −3.6 | 0.9 | 1.2 | 0.8 | 4.7 |
| Vacuolar protein sorting 24 (yeast) | Vps24 | 2.4 | 0.8 | 3.1 | 2.7 | −0.1 | −0.1 | −1.5 | −1.9 |
| Oxidative stress-related genes | | | | | | | | | |
| Activating transcription factor 7 interacting protein 2 | Atf7ip2 | −1.0 | −2.4 | −1.7 | −2.0 | 2.9 | 2.9 | 1.5 | 3.4 |
| Nitric oxide synthase 1 (neuronal) adaptor protein | Nos1ap | 2.8 | 3.2 | 3.6 | 1.6 | −2.4 | −2.4 | −2.4 | −1.7 |
| Superoxide dismutase 2, mitochondrial | Sod2 | 2.4 | 3.6 | 4.4 | 3.4 | −2.8 | −1.6 | −1.4 | −0.3 |
| Cell cycle-related genes | | | | | | | | | |
| Kidney expressed gene 1 | Keg1 | 3.1 | 3.5 | 4.4 | 1.9 | −1.5 | −3.4 | −3.0 | −1.2 |
| Schlafen 1 | Slfn1 | 0.7 | 0.7 | 3.7 | 2.9 | 0.4 | −1.2 | −4.7 | −4.0 |
| Sarcospan | Sspn | −2.1 | −2.4 | −2.0 | −2.8 | 3.5 | 2.9 | 0.6 | 0.0 |
| WAP four-disulfide core domain 1 | Wfdc1 | −1.5 | −2.4 | −2.8 | −2.1 | 1.0 | 0.4 | 1.6 | 1.7 |
| Nervous system development-related genes | | | | | | | | | |
| Calcitonin/calcitonin-related polypeptide, alpha | Calca | −0.7 | −3.9 | −3.0 | −2.9 | −2.2 | 1.6 | 2.5 | 2.4 |
| Galanin | Gal | −2.7 | −2.0 | −2.4 | −2.2 | 0.2 | 1.7 | 0.6 | 1.3 |
| Platelet-activating factor acetylhydrolase isoform1b beta1 | Pafah1b1 | 3.2 | 2.1 | 2.7 | 2.5 | −1.1 | −1.1 | −2.7 | −2.8 |
| Serine (or cysteine) peptidase inhibitor, clade I, member 1 | Serpini1 | 3.0 | 0.7 | 1.9 | 1.8 | −4.9 | −2.6 | −1.4 | −3.9 |
| SRY-box containing gene 3 | Sox3 | 0.1 | −2.5 | −1.0 | −1.3 | 0.6 | 3.7 | 2.2 | 2.3 |
| Inflammatory & immune response-related genes | | | | | | | | | |
| CD8 antigen, beta chain 1 | Cd8b1 | −2.7 | −4.0 | −2.7 | −2.5 | −0.3 | 2.2 | 3.2 | 1.9 |
| Granzyme A | Gzma | 0.7 | 1.5 | 2.6 | 1.6 | 0.4 | −1.8 | −3.3 | −1.5 |
| Interferon activated gene 202B | Ifi202b | −4.5 | −3.6 | −4.6 | −3.9 | 4.1 | 3.3 | 2.2 | 0.2 |
| Interleukin 1 receptor, type I | Il1r1 | 1.4 | 1.3 | 3.0 | 4.0 | 0.6 | 0.1 | −2.6 | −1.8 |
| Toll-like receptor 4 | Tlr4 | 0.5 | 0.2 | 0.2 | −0.1 | −1.5 | −1.1 | −1.7 | −0.9 |
| Angiogenesis-related genes | | | | | | | | | |
| Fibroblast growth factor receptor 2 | Fgfr2 | −2.7 | −2.9 | −2.2 | −4.2 | 3.0 | 1.4 | 2.4 | 4.3 |
| The others | | | | | | | | | |
| aarF domain containing kinase 2 | Adck2 | 2.9 | 3.4 | 5.1 | 3.3 | 0.2 | −1.8 | −5.4 | −3.1 |
| A kinase (PRKA) anchor protein 6 | Akap6 | 0.3 | −2.4 | −3.1 | −2.0 | 0.5 | 2.5 | 2.9 | 1.8 |
| Amyotrophic lateral sclerosis 2 chromosome region, candidate 13 | Als2cr13 | 2.5 | 2.0 | 4.5 | 1.1 | −2.5 | −3.4 | −5.3 | −0.1 |
| Anthrax toxin receptor 2 | Antxr2 | 5.6 | 6.4 | 6.6 | 6.4 | −2.1 | −5.9 | −1.3 | −4.0 |
| UDP-GlcNAc:betaGal beta-1,3-*N*-acetylglucosaminyltransferase 7 | B3gnt7 | −1.5 | −3.5 | −2.5 | −2.4 | 1.1 | 3.3 | 1.6 | 1.8 |
| Procollagen, type IV, alpha 6 | Col4a6 | 2.2 | 2.1 | 2.7 | 2.1 | −2.5 | −2.4 | −4.4 | −1.6 |
| DNA binding protein with his-thr domain | Dbpht2 | −3.7 | −5.2 | −5.0 | −5.3 | 3.5 | 3.3 | 3.9 | 4.4 |
| Ethanolamine kinase 1 | Etnk1 | 0.3 | 0.8 | 2.3 | 2.2 | −3.7 | −2.5 | −3.1 | −2.3 |
| Grancalcin | Gca | −0.8 | −4.9 | −3.5 | −4.9 | −2.8 | 5.6 | 3.2 | 4.0 |
| Gulonolactone (L-)oxidase | Gulo | −2.4 | −3.6 | −5.0 | −3.1 | 2.2 | 2.1 | 5.5 | −0.6 |
| Kinesin family member 21A | Kif21a | −3.6 | −2.9 | −4.7 | −2.3 | 2.1 | 1.4 | 4.5 | 2.2 |
| Lens intrinsic membrane protein 2 | Lim2 | −2.6 | −2.3 | −2.5 | −2.8 | 0.3 | 1.1 | 1.7 | 2.2 |
| Melanoma antigen, family B, 5 | Mageb5 | −2.1 | −1.4 | −2.2 | −2.4 | 0.8 | 2.0 | 2.4 | 2.9 |
| Outer dense fiber of sperm tails 1 | Odf1 | −3.7 | −3.5 | −3.4 | −3.2 | 1.1 | 3.0 | 2.4 | 2.9 |
| Pore forming protein-like | Pfpl | −3.7 | −2.2 | −2.1 | −2.7 | 4.1 | 1.6 | 2.5 | 4.1 |
| Prion protein interacting protein 1 | Prnpip1 | −2.6 | −3.1 | −2.7 | −2.3 | 2.7 | 2.9 | 1.1 | 1.5 |
| Quaking | Qk | 2.7 | 2.4 | 2.7 | 2.6 | −0.6 | −1.7 | −3.8 | −1.9 |
| Villin 1 | Vil1 | −3.4 | −1.2 | −1.4 | −2.9 | 3.3 | 2.5 | 2.0 | 3.9 |
| Proteolysis-related genes | | | | | | | | | |
| Mastermind like 2 (Drosophila) | Maml2 | 2.1 | 1.8 | 2.4 | 1.8 | −3.6 | −2.9 | −4.3 | −2.5 |
| Pregnancy-associated plasma protein A | Pappa | −0.2 | −3.5 | −2.7 | −2.7 | −0.6 | −0.5 | 2.5 | 3.7 |
| Plasma glutamate carboxypeptidase | Pgcp | 3.5 | 3.3 | 4.0 | 2.9 | −2.8 | −1.1 | −1.6 | −2.8 |
| Plasminogen | Plg | 0.8 | 2.0 | 2.8 | 2.6 | 0.1 | −1.1 | −1.9 | −3.3 |
| Protein C | Proc | 1.7 | 2.9 | 2.2 | 2.4 | −1.5 | −3.6 | −3.9 | −1.1 |
| Protease, serine, 3 | Prss3 | 4.1 | 5.0 | 4.9 | 3.5 | −0.2 | −3.3 | −2.1 | −2.4 |

*a*) Compared to untreated BV-2 microglial cells incubated for the same time.

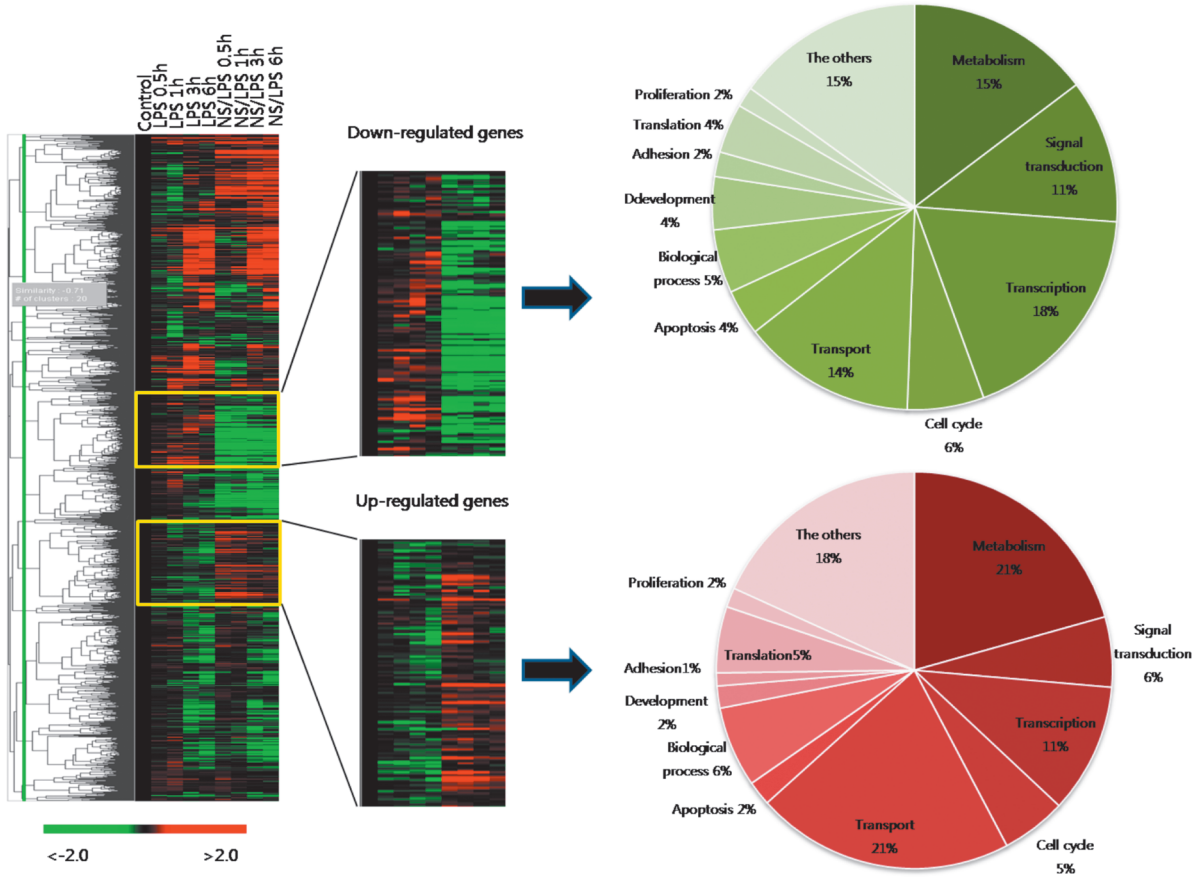


Fig. 4. Clustergram of Up- and Down-Regulated Gene in BV-2 Microglial Cells

Microarray data from control (non-treated BV-2 microglial cells) and experimental (LPS or LPS plus NS-treated BV-2 microglial cells) group were combined and clustered. This indicates that there are 3 independent samples for each treatment. Each gene is represented by a single row of clustered boxes; each experimental sample is represented by a single column. The entire clustered image is shown on the left. These clusters contain uncharacterized genes and genes not involved in these processes. The functional categories of up- and down-regulated genes are shown on the right.

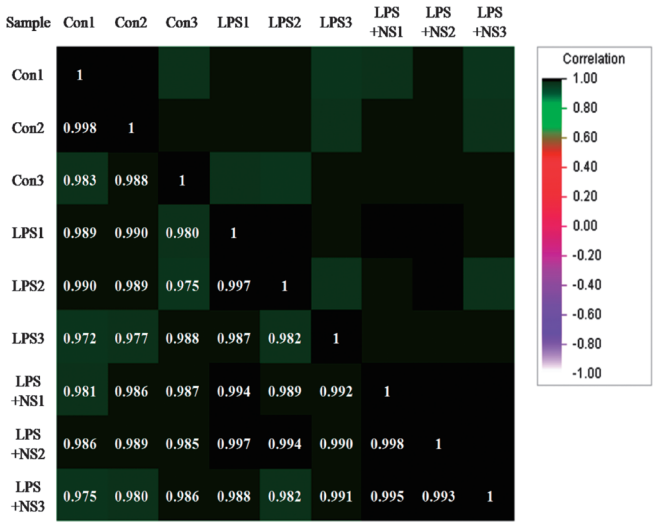


Fig. 5. Correlation Matrix Plot Analysis to Calculate Reproducibility between Triplicates

NS should read NS/LPS since the cells were first treated with NS and then stimulated with LPS. The $R^2$ value calculation is based on intensity signals from all probe sets on the Affymetrix Mouse 430 2.0 array. Based on $R^2$, the microarray hybridization patterns were highly consistent among the sample. A perfect relationship among the samples would produce a slope of 1.

Different types of mitochondrial metabolism, such as oxidative phosphorylation and ATP generation, are emerging as key factors in the generation of ROS associated with a large number of disease states including atherosclerosis, Alzheimer's disease, Parkinson's neuronal death, acute and chronic degenerative cardiac myocyte death, and cancer.[28] In this experiment, NS was found to regulate mitochondrial related signaling pathways such as oxidative phosphorylation, the citrate cycle, proteasomes, one carbon pool by folate, and ATP synthesis. In addition, we observed alterations in genes related to brain diseases such as Huntington's disease (Table 2). Taken together, these results suggest that NS would be an effective therapeutic approach to alleviating the progression of neurodegenerative diseases.

In addition, we found specific and significant alterations of the expression profile of NS-treated BV-2 microglial cells (Table 1). The cellular processes represented by these genes include inflammatory and immune response (Toll-like receptor 4 (*Tlr4*), CDC91 cell division cycle 91-like 1 (*Cdc91l1*), phosphatidylinositol glycan anchor biosynthesis, class Q (*Pigq*)), signal transduction (fibroblast growth factor receptor 3 (*Fgfr3*), *Fgf12*, RAS protein activator like 2 (*Rasal2*), nuclear factor of kappa light polypeptide gene enhancer in B-cells 2, p49/p100 (*Nfkb2*), nuclear factor of activated T-cells, cytoplasmic, calcineurin-dependent 2 (*Nfatc2*), mitogen activated protein kinase 1 (*Mapk1*), *Map2k5*, and *Map3k7*), and

Table 2. Regulation of Pathway Based on Comparison of Gene Expression between LPS Plus *Nelumbinis semen*-Treated and LPS-Treated BV-2 Cells

| KEGG pathway | Gene counts | *p*-Value |
|---|---|---|
| Down-regulated pathway | | |
| Regulation of actin cytoskeleton | 44 | 0.000 |
| Insulin signaling pathway | 34 | 0.000 |
| Huntington's disease | 12 | 0.001 |
| Starch and sucrose metabolism | 14 | 0.002 |
| Cell cycle | 26 | 0.003 |
| Inositol phosphate metabolism | 14 | 0.003 |
| B cell receptor signaling pathway | 18 | 0.004 |
| Wnt signaling pathway | 33 | 0.005 |
| Adherens junction | 22 | 0.010 |
| Focal adhesion | 38 | 0.011 |
| mTOR signaling pathway | 14 | 0.012 |
| *O*-Glycan biosynthesis | 6 | 0.012 |
| Apoptosis | 19 | 0.014 |
| Tight junction | 26 | 0.015 |
| Phosphatidylinositol signaling system | 16 | 0.015 |
| Hedgehog signaling pathway | 13 | 0.024 |
| Jak-STAT signaling pathway | 24 | 0.028 |
| T cell receptor signaling pathway | 20 | 0.030 |
| Fc epsilon RI signaling pathway | 16 | 0.031 |
| Glycan structures-biosynthesis 1 | 15 | 0.039 |
| Pentose phosphate pathway | 7 | 0.043 |
| Aminosugars metabolism | 7 | 0.047 |
| Up-regulated pathway | | |
| Oxidative phosphorylation | 38 | 0.000 |
| Proteasome | 14 | 0.000 |
| Citrate cycle (TCA cycle) | 12 | 0.000 |
| Purine metabolism | 25 | 0.001 |
| Lysine degradation | 12 | 0.001 |
| One carbon pool by folate | 7 | 0.001 |
| Cyanoamino acid metabolism | 4 | 0.001 |
| Pyrimidine metabolism | 18 | 0.001 |
| Biotin metabolism | 4 | 0.004 |
| Glutathione metabolism | 8 | 0.005 |
| Cell cycle | 20 | 0.005 |
| Fatty acid elongation in mitochondria | 4 | 0.005 |
| Protein export | 5 | 0.006 |
| Basal transcription factors | 7 | 0.008 |
| Methane metabolism | 4 | 0.012 |
| Methionine metabolism | 5 | 0.013 |
| RNA polymerase | 6 | 0.019 |
| Reductive carboxylate cycle ($CO_2$ fixation) | 4 | 0.030 |

oxidative stress (nitric oxide synthase 1 (neuronal) adaptor protein (*Nos1ap*)).

The responses to LPS are the result of activation of monocytes, macrophages and neutrophils. Activation of these cells requires binding of LPS to the glycosyl phosphoinositol anchored molecule, CD14. Signaling of the LPS-CD14 complex through the TLR4 to activate the NF-$\kappa$B and MAPK pathways.[29—31] In this study, we detected the down-regula-

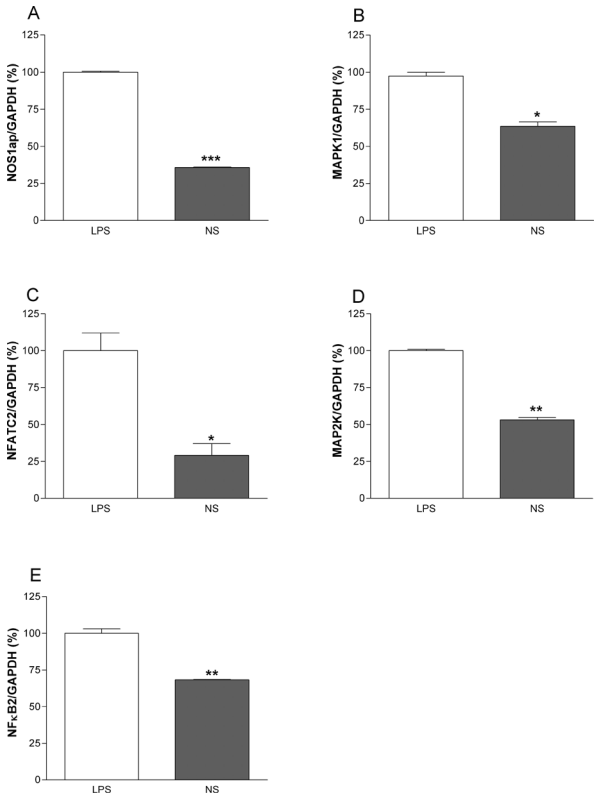


Fig. 6. Effects of *Nelumbinis semen* on mRNA Levels Determined by Real-Time RT-PCR

(A) Nos1ap, (B) MAPK1, (C) NFATC2, (D) MAP2K5 and (E) NF$\kappa$B2, LPS: control. Data are presented as mean±S.E.M. $*p<0.05$, $**p<0.01$, and $***p<0.001$ compared to control; $n=3$ (each group).

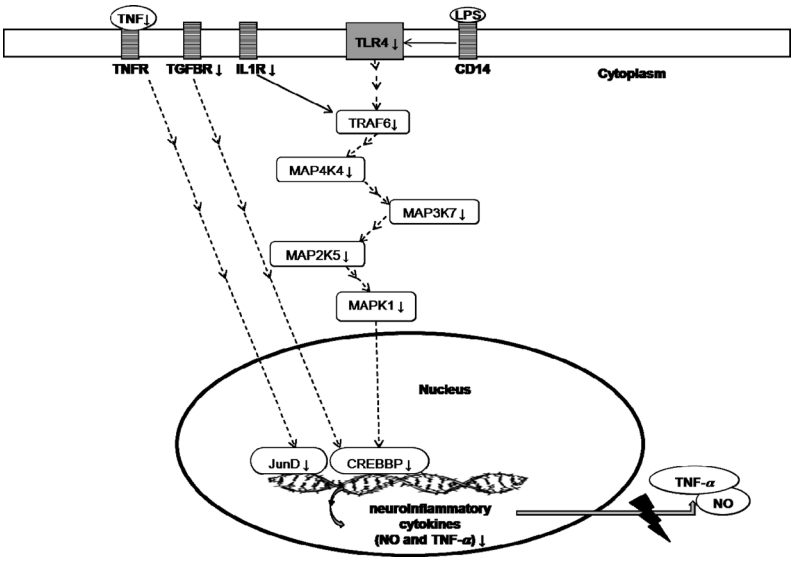


Fig. 7. *Nelumbinis semen* Mediated Anti-neuroinflammatory Pathway

↓ Down-regulation.

tion of *Cdc91l1*, *Pigq*, and *Tlr4* in NS-treated BV-2 microglial cells (Table 1). The MAPK pathways are deeply involved in signaling for various immune responses including apoptosis. MAPKs are serine/threonine kinases, which include the extracellular signal-related kinases (ERKs), p38 kinases, and c-Jun *N*-terminal kinases (JNKs). Activation of the MAPK pathway often occurs in response to growth factor stimulation of receptor tyrosine kinases, which are coupled to the activation of Ras G-proteins through Src homology 2 domain-containing proteins, such as Shc and Grb2, and quinine nucleotide exchange factors such as SOS.[32, 33] In this study, we detected the down-regulation of *Fgfr3*, *Fgf12*, *Rasal2*, *Nfkb2*, *Nfatc2*, *Mapk1*, *Map2k5*, and *Map3k7* in NS-treated BV-2 microglial cells (Table 1, Figs. 6B—E). Each of the MAPKs have also been implicated in neuroinflammatory events, including mediation of many of the physiological responses to NO. For example, NO regulation of matrix metalloproteinases proteins, including MMP1, during inflammatory and angiogenic responses may require MAPK proteins. NO is a signaling molecule, neurotransmitter, and immune effector.[5,32,34] As shown by the ELISA data, NO production was significantly inhibited by 1 $\mu$g/ml NS (Fig. 1). NO is produced by the activity of the family of enzymes nitric-oxide synthases (NOSs), and the *Nos1ap* gene encodes a cytosolic protein that binds to the signaling molecule, neuronal nitric oxide synthase (nNOS). This protein has a *C*-terminal PDZ-binding domain that mediates interactions with nNOS and an *N*-terminal phosphotyrosine binding domain that binds to the small monomeric G protein, Dexras1. Studies evaluating related mouse and rat proteins have shown that this protein functions as an adapter protein linking nNOS to specific targets, such as Dexras1 and the synapsins.[35] In this study, we found that *Nos1ap* was down-regulated in NS-treated BV-2 microglial cells (Table 1, Fig. 6A).

The *TNF-$\alpha$* gene encodes a multifunctional proinflammatory cytokine that belongs to the TNF superfamily. This cytokine, which is primarily secreted by macrophages, can bind to and function through its receptors for TNFRSF1A/TNFR1 and TNFRSF1B/TNFBR. TNF-$\alpha$ is associated with the activation of inflammatory signaling, neural cell dysfunction, apoptosis and brain cell death, and has also been implicated in a variety of diseases, including autoimmune diseases, insulin resistance, and cancer. Additionally, knockout studies in mice have suggested that TNF-$\alpha$ deletion exerts a neuroprotective function.[36,37] In this study, ELISA analysis revealed that TNF-$\alpha$ production was significantly inhibited by 1 $\mu$g/ml NS (Fig. 2), which indicates that NS exerts its effects *via* a pathway that protects cells from neuroinflammatory cytokine regulation (Fig. 7).

Taken together, the results of this study suggest that NS may have potential efficacy for the treatment of inflammatory disease and other neurodegenerative diseases through anti-neuroinflammation activity that occurs *via* inhibition of the MAPK pathway.

**Acknowledgements** This work was supported by the Korea Science and Engineering Foundation (KOSEF) grant funded by the Korea government (MEST) (No. R13-2007-019-00000-0).

## REFERENCES

1) Horner P. J., Gage F. H., *Nature* (London), **407**, 963—970 (2000).
2) Ock J., Jeong J., Choi W. S., Lee W. H., Kim S. H., Kim I. K., Suk K., *J. Neurosci. Res.*, **85**, 1989—1995 (2007).
3) Takaki H., Koganemaru R., Iwakawa Y., Higuchi R., Miyamoto T., *Biol. Pharm. Bull.*, **26**, 380—382 (2003).
4) Medzhitov R., *Nature* (London), **454**, 428—435 (2008).
5) Akundi R. S., Candelario-Jalil E., Hess S., Hull M., Lieb K., Gebicke-Haerter P. J., Fiebich B. L., *Glia*, **51**, 199—208 (2005).
6) Kim W. K., Jang P. G., Woo M. S., Han I. O., Piao H. Z., Lee K., Lee H., Joh T. H., Kim H. S., *Neuropharmacology*, **47**, 243—252 (2004).
7) Nagai A., Mishima S., Ishida Y., Ishikura H., Harada T., Kobayashi S., Kim S. U., *J. Neurosci. Res.*, **81**, 342—348 (2005).
8) Rock R. B., Peterson P. K., *J. Neuroimmune. Pharmacol.*, **1**, 117—126 (2006).
9) Seo W. G., Pae H. O., Oh G. S., Chai K. Y., Yun Y. G., Kwon T. O., Chung H. T., *Gen. Pharmacol.*, **35**, 21—28 (2000).
10) Hou R. C., Chen H. L., Tzen J. T., Jeng K. C., *Neuroreport*, **14**, 1815—1819 (2003).
11) Mosley R. L., Benner E. J., Kadiu I., Thomas M., Boska M. D., Hasan K., Laurie C., Gendelman H. E., *Clin. Neurosci. Res.*, **6**, 261—281 (2006).
12) Jang C. G., Kang M., Cho J. H., Lee S. B., Kim H., Park S., Lee J., Park S. K., Hong M., Shin M. K., Shim I. S., Bae H., *Arch. Pharm. Res.*, **27**, 1065—1072 (2004).
13) Kang M., Shin D., Oh J. W., Cho C., Lee H. J., Yoon D. W., Lee S. M., Yun J. H., Choi H., Park S., Shin M., Hong M., Bae H., *Am. J. Chin. Med.*, **33**, 205—213 (2005).
14) Sohn D. H., Kim Y. C., Oh S. H., Park E. J., Li X., Lee B. H., *Phytomedicine*, **10**, 165—169 (2003).
15) Jung H. A., Jung Y. J., Yoon N. Y., Jeong D. M., Bae H. J., Kim D. W., Na D. H., Choi J. S., *Food Chem. Toxicol.*, **46**, 3818—3826 (2008).
16) Sohn S. H., Ko E., Kim Y., Shin M., Hong M., Bae H., *Mol. Cell. Toxicol.*, **4**, 113—123 (2008).
17) Kim J., Lee H., Lee Y., Oh B. G., Cho C., Kim Y., Shin M., Hong M., Jung S. K., Bae H., *J. Ethnopharmacol.*, **114**, 186—193 (2007).
18) Chung H. S., Kang M., Cho C., Parvez S., Park C. H., Kim D., Oh J., Kim H., Shin M., Hong M., Kim Y., Bae H., *Biol. Pharm. Bull.*, **30**, 912—916 (2007).
19) Kim C. S., Sohn S. H., Jeon S. K., Kim K. N., Ryu J. J., Kim M. K., *J. Oral. Rehabil.*, **33**, 368—379 (2006).
20) Wang Y., Barbacioru C., Hyland F., Xiao W., Hunkapiller K. L., Blake J., Chan F., Gonzalez C., Zhang L., Samaha R. R., *BMC Genomics*, **7**, 59 (2006).
21) Saura J., Tusell J. M., Serratosa J., *Glia*, **44**, 183—189 (2003).
22) Lim S. S., Jung Y. J., Hyun S. K., Lee Y. S., Choi J. S., *Phytother. Res.*, **20**, 825—830 (2006).
23) Sugimoto Y., Furutani S., Itoh A., Tanahashi T., Nakajima H., Oshiro H., Sun S., Yamada J., *Phytomedicine*, **15**, 1117—1124 (2008).
24) Liu C. P., Kuo Y. C., Shen C. C., Wu M. H., Liao J. F., Lin Y. L., Chen C. F., Tsai W. J., *J. Leukoc. Biol.*, **81**, 1276—1286 (2007).
25) Lobell M., Molnar L., Keseru G. M., *J. Pharm. Sci.*, **92**, 360—370 (2003).
26) Reynolds A. D., Kadiu I., Garg S. K., Glanzer J. G., Nordgren T., Ciborowski P., Banerjee R., Gendelman H. E., *J. Neuroimmune. Pharmacol.*, **3**, 59—74 (2008).
27) Skaper S. D., *Ann. N. Y. Acad. Sci.*, **1122**, 23—34 (2007).
28) Hoye A. T., Davoren J. E., Wipf P., Fink M. P., Kagan V. E., *Acc. Chem. Res.*, **41**, 87—97 (2008).
29) Leon-Ponte M., Kirchhof M. G., Sun T., Stephens T., Singh B., Sandhu S., Madrenas J., *Immunol. Lett.*, **96**, 73—83 (2005).
30) Jiang Y., Chen G., Zheng Y., Lu L., Wu C., Zhang Y., Liu Q., Cao X., *Mol. Immunol.*, **45**, 1557—1566 (2008).
31) Aravalli R. N., Peterson P. K., Lokensgard J. R., *J. Neuroimmune. Pharmacol.*, **2**, 297—312 (2007).
32) Raines K. W., Cao G. L., Porsuphatana S., Tsai P., Rosen G. M., Shapiro P., *J. Biol. Chem.*, **279**, 3933—3940 (2004).
33) Sim S., Yong T. S., Park S. J., Im K. I., Kong Y., Ryu J. S., Min D. Y., Shin M. H., *J. Immunol.*, **174**, 4279—4288 (2005).
34) Zaragoza C., Soria E., Lopez E., Browning D., Balbin M., Lopez-Otin C., Lamas S., *Mol. Pharmacol.*, **62**, 927—935 (2002).
35) Fang M., Jaffrey S. R., Sawa A., Ye K., Luo X., Snyder S. H., *Neuron*, **28**, 183—193 (2000).
36) Boetkjaer A., Boedker M., Cui J. G., Zhao Y., Lukiw W. J., *Neurosci. Lett.*, **426**, 59—63 (2007).
37) Fakhrzadeh L., Laskin J. D., Laskin D. L., *Toxicol. Appl. Pharmacol.*, **227**, 380—389 (2008).